FRACTURE MECHANICS OF SPALLING CRACKS IN COLD WORK ROLLS

T. Mizoguchi*, K. Yoshikawa* and S. Ohta*

* Central Research Laboratory,
Kobe Steel Ltd., Kobe, Japan

ABSTRACT

The mechanism of the spalling failure of work rolls for cold rolling mills was analyzed considering crack propagation behavior under combined mode stress intensity factors caused by contact stress and compressive residual stress. It was assumed that in compression, the crack is closed, and thus, K_I can not contribute to crack propagation, but the material can still fail because of the maximum tensile stress around the crack tip due to the existence of K_{II} . The magnitude of tensile stress intensities at the crack tip was calculated considering crack angles, residual stress, contact stress and friction between the crack faces. It was shown that the results of the analysis, together with the measurement of fracture characteristic of the material, can explain the actual crack behavior to some extent. Through these analyses, the effects of the applied load and residual stress on the spalling crack behavior and critical crack size were evaluated.

KEYWORDS

Cold work roll; Spalling; Combined modes; Compression; Contact stress; Residual stress; Brittle material

INTRODUCTION

The spalling or cracking-out of significantly large pieces from hardened outer layer of the work rolls is one of the most serious problems encountered in cold strip mills and a major concern to users and manufacturers of the rolls.
Cold work rolls are often subjected to thermal shock on their surface as a result of the slip between the work roll and the back up roll or the strip due to poor operation of the mill. Since the hardened outer layer of work roll has a hardness of 750 Hv or more and contains more than 0.8% carbon for the purpose of wear resistance, it is significantly sensitive to thermal shock and heat cracks can occur easily on or near the surface.
Usually, after the use of rolls, the surface is examined and ground off to detect and remove the damaged layer by thermal shock. However, the possibility of overlooking microcracks is present in some of these procedures.

In what follows, and so as to clarify the mechanical and metallurgical factors

that control the failure process, a more quantitative analysis is carried out for the stage of crack propagation from unremoved micro heat cracks.

FRACTURE APPEARANCE

Fig.1 shows a typical spalling appearance of a cold work roll. Fig.2 shows the cross sectional view of spalling crack propagation. Usually, the crack starts from the surface and extends in a circumferential direction at an angle of about 20 to 40 degrees to the roll surface. After the crack reaches the boundary between the hardened layer and the core, it progreses in a circular path parallel to the roll surface. During the crack propagation, the width of the crack is kept constant, and hence a band-like fracture surface with a series of "thumb nail" marks is formed as shown in Fig.3. When the band-like crack orbits one or two times round the roll, the catastrophic breaking-out is initiated probably due to the radial tensile residual stress.

It has become apparent that intergranular fracture, although crashed by compressive stress, occurs on the band-like fracture surface in the vicinity of the crack origin and on the side region of the thumb nail marks as shown in Fig.3. The fracture mode of other parts of band-like fracture surface and final fracture surface, was defined as transgranular fracture.

FRACTURE MECHANICS APPROACH

Model for Analysis

The following model was selected to carry out an analysis for the stage of spalling crack propagation from an initial thermal crack that had not been removed by re-grinding. The crack was assumed to be a half elliptical surface crack with the major semiaxis of C that inclines in a circumferential direction at an angle of β, and the minor semiaxis of a that is on the surface and parallel to the longitudinal direction of the roll as shown in Fig.4. The crack is subjected to contact stress due to the rolling operation and the residual stress provided during the surface hardening process. These stresses can be resolved into two components, the normal stress σ_n perpendicular to the crack plane and the shear stress τ_s parallel to the crack plane. The values of σ_n and τ_s are the functions of the distance from the contact point. It is also possible that the crack faces are subjected to the hydraulic pressure p caused by pressurized lubricant. As shown later, the value of the compressive residual stress in the circumferential direction is so great that σ_n is almost compression. Therefore, the problem can be reduced to that of crack propagation under combined mode stress intensities in compressive stress field.

In the limit of $a/C \to \infty$, the subject can be simplified to 2 dimensional problems of angled edge crack. Because the general solution of K_I and K_{II} for the angled edge crack under non-uniform stress field has not been obtained, it was assumed that K_I and K_{II} are equal to those of not angled edge crack subjected to the same distributed normal and shear stress on the crack plane. Based on the above assumption, mode I and mode II stress intensity factors $K_{I\infty}$, $K_{II\infty}$ of the edge crack in the limit of $a/C \to \infty$ are

$$K_{I\infty} + iK_{II\infty} = 2\int_0^1 (\sigma_n + p + i\,\tau_{se})\,(1 + F(\xi))\sqrt{\frac{\pi C}{1-\xi^2}}\,d\xi \qquad (1)$$

Where F is a function of the normalized distance from the edge (Hartranft, 1973) (see Fig.4). In compressive stress field, the friction between the crack faces

should be taken into account. Subtraction of the frictional component from the shear stress τ_s gives an effective shear stress τ_{se} (Melville, 1977).

$$|\tau_{se}| = |\tau_s| - \mu|\sigma_n + p| \quad , \quad (|\tau_s| > \mu|\sigma_n + p|) \qquad (2)$$

Where μ is the frictional coefficient. If $|\tau_s|$ is smaller than $\mu|\sigma_n + p|$, τ_{se} can be assumed to be 0.

In order to calculate the value of K_I and K_{II} of the half elliptical crack shown in Fig.4, it was assumed that the effect of the ratio of the crack width $2a$ to length C on the stress intensity factors along the crack border is the same as that in the problem of the infinite solid containing an elliptical crack solved by Kassier and Sih (1966). The assumption leads to the results for K_{II} in case of $C > a$ as

$$K_{II} = \frac{k'k^2}{(k^2 - \nu)\,E(k) + \nu k'^2\,K(k)}\cos\varphi \cdot K_{II\infty} \qquad (3)$$

where

$$k = \sqrt{1-(a/C)^2} \quad , \quad k' = a/C \, ,$$

K_{II} for $C < a$ and K_I were also obtained in the same way.

Fracture Criterion in Compression

Several investigators (Cotterell, 1972; Hoek, 1965) have undertaken the fracture criterion of brittle material with cracks in compression. Unfortunately, however, the cracks examined in these investigations have been limited to open cracks. Therefore, it seems that the fracture criterion for closed cracks has not been established. But on the basis of these investigations and other studies on combined mode brittle fracture (Erdogan, 1963; Tirosh, 1977), it may be concluded that the maximum tensile stress around the crack is a dominant factor.

Therefore, it was assumed that the crack will start to extend in the plane which is normal to the maximum circumferential stress $\sigma_{\theta\max}$ (Fig 4), that is

$$\sigma_{\theta\max} = \frac{1}{\sqrt{2\pi r}}\cos\frac{\theta_0}{2}\left[K_I\cos^2\frac{\theta_0}{2} - \frac{3}{2}K_{II}\sin\theta_0\right] \qquad (4)$$

where θ_0 is the initial angle of crack growth and it has to satisfy the following equation.

$$K_I\sin\theta_0 + K_{II}\,(3\cos\theta_0 - 1) = 0 \qquad (5)$$

However, in compression, the crack is closed, and thus, K_I can not contribute to crack propagation. Consequently, in the case of $K_I < 0$, 0 should be substituted to K_I in eq.(4) and eq. (5). Here, as a parameter that represents the tensile stress intensity around the crack tip, K_σ was defined as follow.

$$K_\sigma = \cos\frac{\theta_0}{2}\left[K_I\cos^2\frac{\theta_0}{2} - \frac{3}{2}K_{II}\sin\theta_0\right] \qquad (6)$$

The value of K_σ varies with the distance between the location of the crack and the contact point. As the maximum value of K_σ during the rotation of the roll, $K\sigma\max$ was defined.

Contact Stress Field

In calculating $K\sigma max$, it is necessary to determine the distribution of each stress component $\sigma n, \tau s$ caused by rolling force and residual stress. The contact stress field can be calculated by integrating the solution for concentrated normal and tangential force, according to the distribution of normal pressure due to rolling force and shearing force due to the friction on the contacting boundary (Czyzewski, 1975; Poritsky, 1950). Fig. 5 shows an example of calculated contact stress distribution produced by contact between work roll and back-up roll with a coefficient of friction $\mu_0 = 0.1$. In case of contact between roll and strip, the stress field can be calculated in a similar manner provided a suitable distribution of rolling pressure and friction is assumed.

Residual Stress Distribution

A high level residual stress is an intrinsic characteristic of the forged and hardened work roll.
The distribution curves of residual stress components are strongly correlated to the hardness distribution curve that can be controlled by the process of heat treatment. In order to clarify the effects of residual stress on the spalling behavior, two examples for distribution curves were selected as shown in Fig.6. One has a steep drop on the hardness distribution curve and hence has high level residual stress of -940 MN/m at the surface (CASE I). In the other case (CASE II), the curve is more gentle and the residual stress at the surface is of 800 MN/m , lower than in CASE I.

RESULTS AND DISCUSSION

Effects of crack angle

As an example, let's consider a case where the work roll contacts the back-up roll under the conditions shown in Fig.7. Where P max is the Hertzian maximum pressure. Fig.7 shows the effects of the inclination angle of crack β on the relationship between $K\sigma max$ and crack length .
$K\sigma max$ increases with increasing C until C reaches half the width of the crack $a = 20$ mm. The magnitude of $K\sigma max$ no longer increases if C exceeds a. It is because the reduction of K_{II} with respect to the increase of C/a is significant in case of $C>a$. It can be seen that the crack angle β that gives the maximum value of $K\sigma max$ ranges from 30 to 35 degrees over the entire range of C.

Needless to say, it is difficult to estimate the crack path completely, because after the crack propagates to the direction of the maximum tangential stress at the crack tip, it is necessary to obtain the stress intensity factor at the end of the branch in compressive stress field which in general is complex. However, from the results on Fig.7, it can be concluded that the crack that inclined to the roll surface at an angle of from 30 to 35 degrees can easily continue to propagate irrespective of its length. This result agrees with the fact that in the hardened outer layer, the actual band-like crack progresses in a circumferential direction at an angle of about 20 to 40 degrees to the roll surface.

It should be also pointed out that it is difficult for the crack to propagate to the transverse direction ($\varphi=90°$ in Fig.4), because at the side of the crack, K_{II} becomes 0 according to eq. (3). This may be the reason why the band-like crack propagates keeping its width constant as shown in Fig.1 or Fig.3.

The relationship between $K\sigma max$ and β is plotted in Fig.8 as a function of μ for different crack length C, showing that $K\sigma max$ depends strongly on μ as well as β. It was also found that β which gives the maximum on the $K\sigma max$-β curve, is shifted from 30 to 45 degrees as μ decreases from 0.4 to 0. This means that the larger the value of the coefficient of friction between the crack faces μ is, the crack can propagate at the more shallow angle.
In such a case that μ equals 0, β-$K\sigma max$ curves take the maximum value at about 40 to 45 degrees. From the facts described above, it can be concluded that the spalling cracks can continue to propagate at an angle less than 45 degrees.

Effects of Residual Stress and Applied Load

$K\sigma max$ at specific β that gives the maximum $K\sigma max$ is plotted in Fig.9 as a function of crack length for different value of residual stress $\sigma_{R\theta}$ at the roll surface and the maximum Herzian pressure P max. It can be seen that the effect of P max in the range of 780 to 1370 MN/m , under which condition the usual operation is carried out is not so significant compared to the effect of residual stress. Even if Pmax equals 0, the value of $K\sigma max$ is considerably large compared to the value of K_{IC} or K_{IS} that will be presented subsequently. Consequently, it is possible that the spalling crack propagation takes place without rolling force. Actually, some of the spalling accidents occur out of operation. It seems important to reduce the residual stress by making the hardness distribution curve more gentle than that of CASE II in Fig.6.

Material Properties

The influence of alloying elements and heat treatment procedures on fracture characteristic of roll material was also investigated. The specimens for K_{IC} test were heat-treated to have a hardness of 700 to 800 H_V as same as in the hardened layer of work rolls. In all specimen, subcritical crack growth was observed prior to unstable crack growth during K_{IC} tests. This subcritical crack growth associates with delayed fracture in air and the crack propagates slowly along the grain boundaries leaving intergranular fracture surface, the features of which are the same as of that observed on the band-like fracture surface of the spalled roll

The stress intensity factor at which subcritical crack growth starts was given the symbol K_{IS}. Fig.10 shows the relationship between the hardness and K_{IS} or K_{IC} of 0.85C-3.5Cr steel commonly used for cold work rolls. It is understandable by comparing Fig.10 with Fig.9 and from the observations described above that the crack which exceeds 0.2 mm or so in length starts as delayed fracture forming the intergranular fracture surface and ends up to catastrophic spalling.
Therefore, non-destructive testing should be done to detect and remove the very small cracks on or near the surface prior to use. It is also desirable to decrease the hardness so far as the wear resistance is kept at a certain level.

CONCLUSIONS

A fracture mechanics analysis was carried out for the stage of spalling crack propagation of cold work rolls based on the assumption that the maximum tensile stress around the crack tip due to mode II stress intensity factor controls the fracture in compression. The following conclusions were obtained.

1) The effects of residual stress, contact stress and friction between the crack faces were evaluated together with the measurements of fracture characteristic of material. The results can explain the actual crack behavior to a certain extent.

2) Because the high level compressive residual stress at the roll surface has a harmful effect on spalling, rolls which have gentle hardness distribution curve should be manufactured to reduce the residual stress. It is also desirable to decrease the surface hardness to prevent spalling accidents.

3) Non destructive testing should be done to detect and remove cracks of less than 0.2 mm length, because very small cracks can start as a delayed fracture and lead to spalling.

REFERENCES

Cotterell, B. (1972). Brittle fracture in compression. Int. J. of Fracture Mech., 8, 195-208

Czyzewski, T. (1975). Influence of a tension stress field introduced in the elastohydrodynamic contact zone on rolling contact fatigue. Wear, 34, 201-214.

Erdogan, F., G.C. Sih. (1963). On the crack extension in plates under plane loading and transvers shear. Trans. ASME, J. of Basic Engs., 85D, 519-527.

Hartranft, R.J., G.C. Sih (973). Methods of analysis and solutions of crack problems. In G.C. Sih (Ed.), Handbook of stress-Intensity factors, Lehigh University, PP 1.3.1-5

Hoek, E., Z.T. Bieniawski. (1965). Brittle fracture propagation in rock under compression. Int. J. of Fracture Mech., 3, 137-155.

Kassir, M.K., G.C. Sih. (1966). Three-dimensional stress distribution around an elliptical crack under arbitrary loadings. Trans. ASME. J of Applied Mech., 601-611.

Melville, P.H. (1977). Fracture mechanics of brittle materials in compression. Int. J. of Fracture, 13, 532-534.

Poritsky, H., N.Y. Schenectady. (1950). Stress and deflections of cylindrical bodies in contact with application to contact of gears and locomotive wheels. Trans. ASME, J. of applied Mech., 191-201.

Tirosh, J. (1977). Incipient fracture angle, fracture loci and critical stress for mixed mode loading. Engng Fracture Mech., 9, 607-616

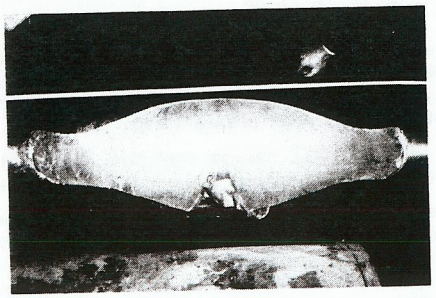

Fig. 1. Appearance of major spall on work roll.

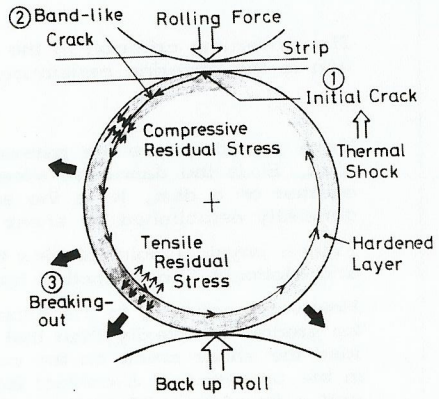

Fig. 2. Cross sectional view of spalling.

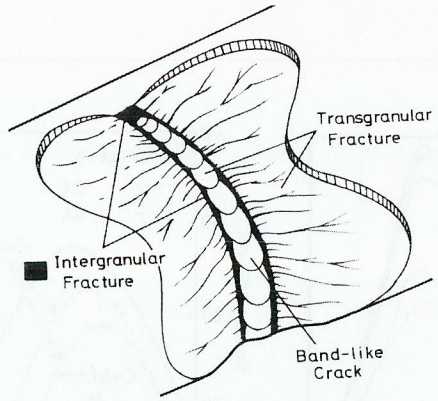

Fig. 3. Schematic diagram showing band like crack propagation.

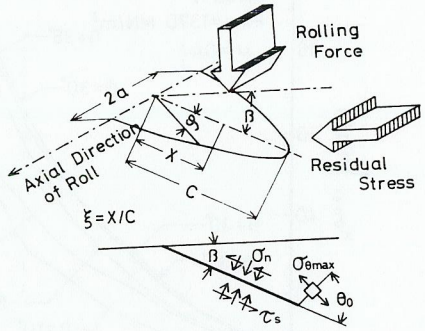

Fig. 4. Stresses acting upon a crack inclined at an angle β.

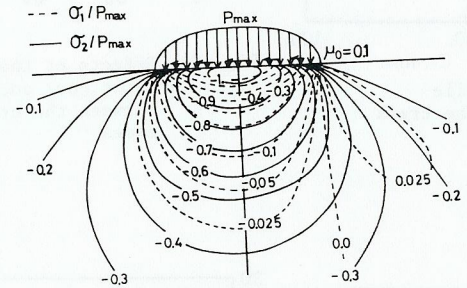

(a) Contours of maximum and minimum principal stresses σ_1, σ_2.

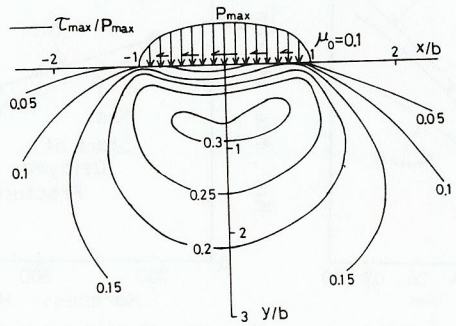

(b) Contours of maximum shear stress τ_{max}.

Fig. 5. Contact stress field.

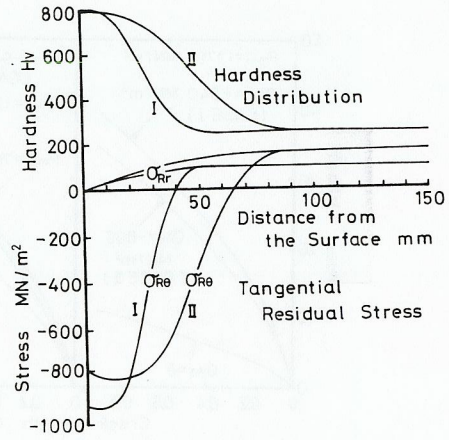

Fig. 6. Hardness and residual stress distribution.

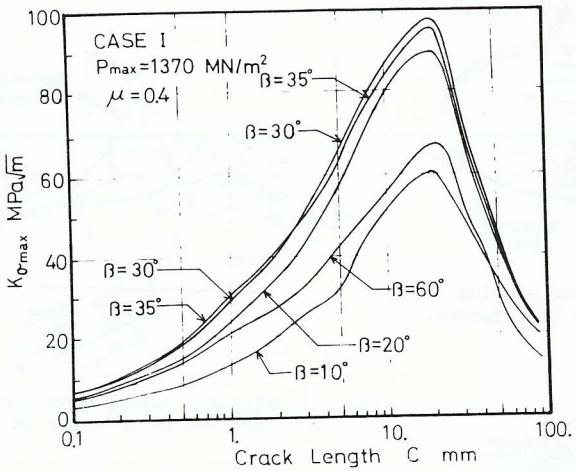

Fig. 7. Relationship between tensile stress intensity around the crack tip and crack length.

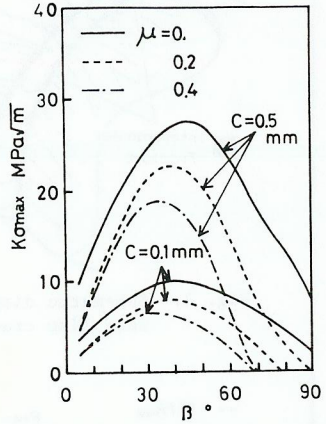

Fig. 8. Effects of the frictional coefficient between the crack faces

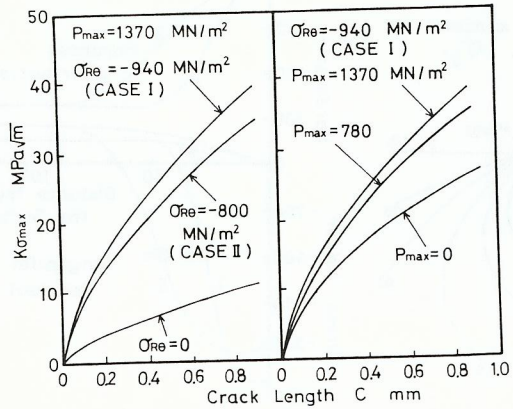

Fig. 9 Effects of contact stress and residual stress.

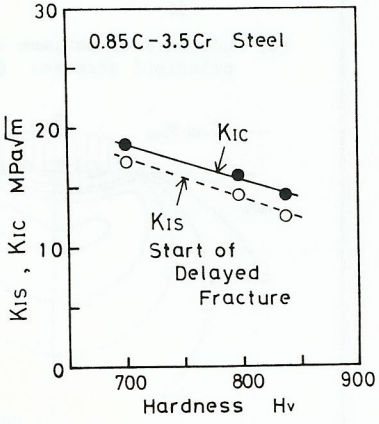

Fig. 10. Relationship between hardness and fracture characteristic of material.